OPEN

Correspondence and
requests for materials
should be addressed to
T.W. (t.wang@
sheffield.ac.uk)

Room temperature plasmonic lasing in a continuous wave operation mode from an InGaN/GaN single nanorod with a low threshold

Y. Hou, P. Renwick, B. Liu, J. Bai & T. Wang

Department of Electronic and Electrical Engineering, University of Sheffield, Mappin Street, Sheffield, S1 3JD, United Kingdom.

It is crucial to fabricate nano photonic devices such as nanolasers in order to meet the requirements for the integration of photonic and electronic circuits on the nanometre scale. The great difficulty is to break down a bottleneck as a result of the diffraction limit of light. Nanolasers on a subwavelength scale could potentially be fabricated based on the principle of surface plasmon amplification by stimulated emission of radiation (SPASER). However, a number of technological challenges will have to be overcome in order to achieve a SPASER with a low threshold, allowing for a continuous wave (cw) operation at room temperature. We report a nano-SPASER with a record low threshold at room temperature, optically pumped by using a cw diode laser. Our nano-SPASER consists of a single InGaN/GaN nanorod on a thin SiO_2 spacer layer on a silver film. The nanorod containing InGaN/GaN multi-quantum-wells is fabricated by means of a cost-effective post-growth fabrication approach. The geometry of the nanorod/dielectric spacer/plasmonic metal composite allows us to have accurate control of the surface plasmon coupling, offering an opportunity to determine the optimal thickness of the dielectric spacer. This approach will open up a route for further fabrication of electrically injected plasmonic lasers.

Electronic integrated circuits face increasing challenges for current communication and computation technologies due to their limits in fundamental speed and bandwidth. Further improvement requires an integration of photonic and electronic circuits on the nanometre scale[1,2]. However, one of the greatest challenges is due to the size incompatibility between electronic and photonic components. Electronic components can be fabricated on a scale of below 100 nm, while there exists a fundamental limit for the fabrication of photonic components as a result of the diffraction limit of light when the dimensions of an optical component approach the wavelength of light. Therefore, the key to achieving this level of integration is to miniaturize photonic components down to the nanometer scale, for instance, nanolasers. In this case, the bottleneck that must be overcome is due to the diffraction limit of light, namely, $\sim\lambda/2n$ limiting the minimal dimension of a laser cavity, where λ and n are the free space wavelength and refractive index, respectively.

One of the most promising approaches of addressing the challenges is to utilise surface plasmons (SPs), which can offer an opportunity to confine light to very small dimensions at a metal/dielectric interface by means of a resonant interaction between the surface electrons in a metal and the electromagnetic fields of light. The confined dimension along the direction perpendicular to the metal/dielectric interface is determined by the decay length of SPs. The decay length of SPs into a metal is typically on the order of 10 nm, two orders of magnitude smaller than the wavelength of light, which paves the way for the fabrication of ultra-small optical components on a subwavelength scale. However, it is worth highlighting that SPs also suffer from losses along their propagation direction. In order to achieve lasing, a sufficiently high gain is required. It has been predicted that ultra-small mode volumes as a result of a plasmonic waveguide would lead to a significant reduction in the propagation loss[3].

Following Bergman and Stockman's proposal on so-called surface plasmon amplification by stimulated emission of radiation (SPASER) in 2003[4], several groups have performed excellent work and then demonstrated optically pumped plamonic lasers using a hybrid plasmonic waveguide in the form of gain material/dielectric/metal[5–9]. These plasmonic lasers all exhibit high thresholds and have been reported to operate under either pulsed optical pumping or continuous wave (cw) optical pumping at low temperatures. It is highly likely that this is due to the use of a single layer (not a heterostructure) as a gain region, causing a low high optical gain. Lu *et al.* recently
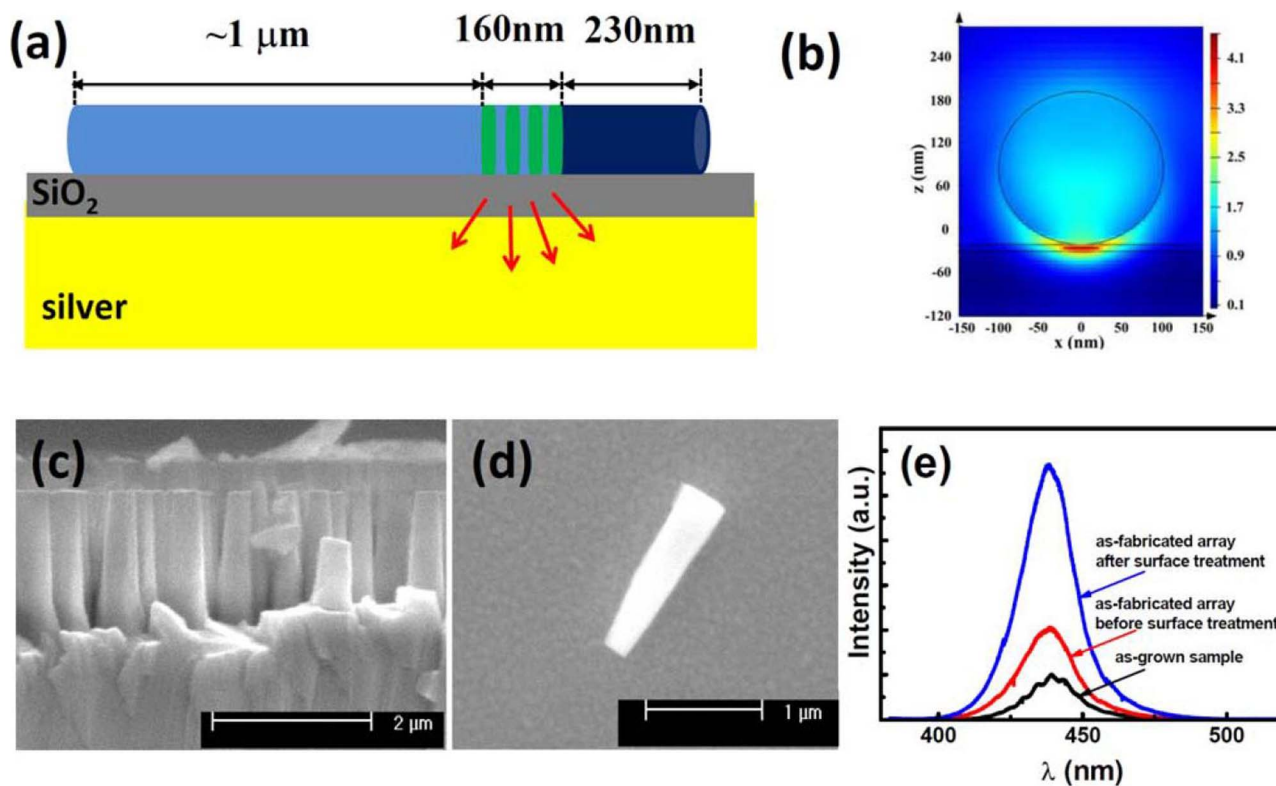
Figure 1 | (a) Schematic diagram of our nano-SPASER; **(b)** Simulated electrical field distribution at the cross-section; **(c)** SEM image of our as-fabricated nanorod array; **(d)** SEM image of an individual nanorods; and **(e)** PL spectra of the nanorod array before and after surface treatment, compared with the as-grown sample.

reported an optically pumped SPASER fabricated using a core-shell InGaN/GaN nanorod, reducing the threshold to 2.1 kW/cm² at 8 K[9], the best report so far. Their plasmonic laser works under an optical pumping in a continuous wave (cw) mode but at low temperatures of up to 78 K only. A number of fabrication challenges need to be overcome in order to further reduce the threshold and achieve a plasmonic laser operating at room temperature in cw mode: 1) A high density of defects may exist in such a core-shell structure as a result of growth on Si substrates by molecular beam epitaxy (MBE)[10]; 2) It might be difficult to achieve excellent mirror facets as a result of the direct growth; 3) The thickness of GaN shell layer could not be controlled accurately, also as a result of the direct growth. This would lead to significant challenges in tuning the separation between the InGaN gain material and the plasmonic metal thus limiting SPs coupling efficiency[11,12]; 4) The core-shell structure used is basically a double heterostructure, and thus the optical gain might not be sufficiently high.

In this paper, we report a nano-SPASER with a very low threshold at room temperature, optically pumped simply using a cw diode laser. Our nano-SPASER consists of a single $In_xGa_{1-x}N/GaN$ nanorod on a thin SiO_2 dielectric layer on a silver film. The nanorod has been fabricated using a standard InGaN/GaN multi-quantum-well (MQW) based a light emitting diode (LED) structure grown on sapphire by metal organic chemical vapor deposition (MOCVD). The MQW and the whole nanorod act as the gain medium and a Fabry-Pérot (F-P) nanocavity, respectively. Compared to the bulk InGaN/GaN core-shell structure, our nanorods containing InGaN/GaN MQWs not only exhibit a high optical gain as a result of increasing density of states, but also allow us to control the separation between the InGaN MQW and the metal accurately. In addition, the nanowire or nanorod based plasmonic nanolasers are basically fabricated from a planar structure, and thus they are perfectly compatible with the current electronic circuits. Furthermore, the mode

area is also smaller than that of the coaxial lasers[13,14], which enables the lasers to conveniently integrate with on-chip optical systems.

All the InGaN/GaN MQW nanorods used in the present study were fabricated from a standard LED epi-wafer by means of a top-down dry etching approach based on our self-organised nickel nano-masks[15]. The length of the nanorods in each case is less than 2 μm, covering a p-GaN layer, a thin p-AlGaN electron-blocking layer, 10 pairs InGaN/GaN MQW (InGaN well: 2.9 nm/GaN barrier: 13.4 nm) as an active region, and part of n-GaN. Subsequently, the nanorods were transferred onto the surface of a 10 nm SiO_2 layer deposited on a silver film in order to form a plasmonic waveguide as schematically shown in Fig. 1a. (See the experimental section and supplementary information for the details of the fabrication). Such a structure allows us to accurately control the separation between the InGaN MQWs and the silver film, which is simply determined by the thickness of the SiO_2 layer. Therefore, it allows us to conveniently tune the exciton-SP coupling between the InGaN MQWs and the silver. Such SP polaritons can be strongly confined to very small dimensions at the interface between the SiO_2 and the silver film, which can be seen clearly from the mode profile given in Fig. 2b. The propagation distance of the SP polaritons in the plasmonic waveguide has been simply estimated, and can be up to tens of micrometres[3,16], which is much longer than the length of the nanor-ods. Consequently, the propagation loss should be significantly reduced. Meanwhile, it is worth highlighting that the optical gain of InGaN/GaN MQWs can be as high as several 1,000 cm⁻¹ in the blue-green region, studied by k•p method[17]. In our case, the gain of the demonstrated laser is estimated to be 3.2×10^3 cm⁻¹ (see the supplementary information), which is two-orders of magnitude higher than that of bulk InGaN[18]. This is due to the significantly higher density of states as a result of InGaN/GaN quantum well structure than that of its bulk counterpart. Furthermore, it is expected that a further reduction in threshold for lasing could be
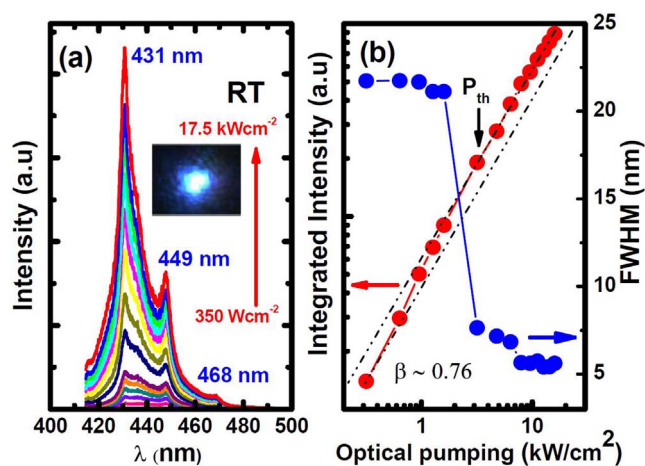
Figure 2 | (a) Lasing spectra from our nano-SPASER recorded as a function of optical pumping at room temperature. Inset showing the far-field laser spot; (b) L-L curve plotted in a log-log scale and FWHM as a function of optical pumping, respectively. The dash-lines are guides to eyes.

Figure 3 | (a) Emission spectra from a InGaN/GaN MQW nanorod on a SiO$_2$ without a silver film underneath recorded as a function of optical pumping at room temperature; (b) L-L curve plotted in log-log scale and FWHM as a function of optical pumping, respectively.

achieved through minimising the scattering of SPs due to the surface roughness and grain boundaries of the silver used. Both the silver film and the thin SiO$_2$ were prepared using a very low deposition rate of less than 1 Å/s under a vacuum of less than 2×10^{-6} mbar. The surface morphology of the thin SiO$_2$ layer on the silver film has been examined using an atomic force microscopy (AFM), exhibiting a root mean square (RMS) roughness of only 1.6 nm in a 5×5 μm^2 scanning area (See the supplementary information).

Fig. 1c displays a typical scanning electron microscopy (SEM) image of our as-fabricated nanorod array structure, demonstrating the fairly straight sidewalls of the nanorods, which could be helpful to reduce any potential optical mode leakage. Fig. 1d shows an individual nanorod which has been transferred onto the surface of the SiO$_2$ over a silver film. The nanorod exhibits a truncated conical shape on the top as a result of the different etching rate between the InGaN region and the n-GaN region. Further optimisation in our dry etching process is still necessary. Here, it is worth noting that we have achieved a pair of well-defined parallel facets, clearly shown in Fig. 1d.

In order to minimise any potential damage or defects (potential non-radiative recombination centres) generated during the dry etching process, a surface treatment was carried out. This process we have developed involves the utilisation of hot nitric acid and has been performed on the nanorods before they are transferred onto the surface of the SiO$_2$ on silver. This surface treatment leads to a massive improvement in optical properties, confirmed by our photoluminescence (PL) measurements as shown in Fig. 1e, where the PL intensity of the nanorods is enhanced by a factor of more than 3. It should be noted that the PL intensity of the nanorods is about 6 times higher than that of the as-grown epi-wafer. The extra PL enhancement compared with the as-grown epi-wafer results from a significant reduction in the lattice-mismatch induced strain as a consequence of fabrication into a nanorod structure, alleviating the strain induced piezoelectric fields across the InGaN/GaN MQWs[19–21]. The reduced piezoelectric fields are also helpful to improve the optical gain of In$_x$Ga$_{1-x}$N/GaN MQW structure[22].

Compared with the previous reports, the design and fabrication of the plasmonic structure stated above offers a significantly enhanced chance for achieving cw lasing with an ultra low threshold at room temperature. Fig. 2a shows room temperature lasing spectra of our plasmonic nanolaser on a 10 nm SiO$_2$ layer deposited on a silver film as a function of optical pumping power density, excited using a standard 405 nm cw diode laser in a micro-PL system. Under low
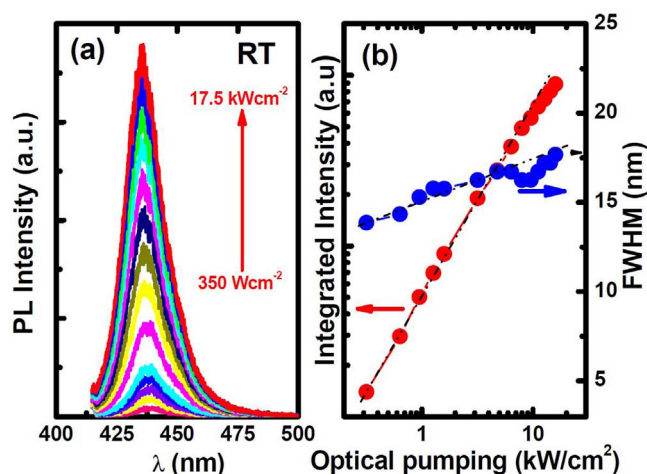
optical pumping power densities only very broad spontaneous emission spectra can be observed. However, above an excitation power density of 3.5 kW/cm^2 the emission intensity increases dramatically. This also corresponds with a significant reduction in full width at half maximum (FWHM) of the peak appearing at 431 nm with increasing optical pumping power density. Fig. 2b shows a light-light (L-L) plot of the lasing mode at 431 nm, described in a log-log scale typically for a plasmonic laser. The L-L curve exhibits an "s" shaped behaviour, a typical fingerprint for lasing. The threshold can be determined from the L-L plot, which is 3.5 kW/cm^2. Fig. 2b also shows the FWHM of the emission peaks as function of optical pumping, exhibiting a dramatic reduction with increasing optical pumping power density which starts from 3.5 kW/cm^2. Eventually, the FWHM drops down to ~6 nm from 22 nm, further confirming the lasing behaviour. The quality factor (Q-factor) can be evaluated from Q = $\lambda/\Delta\lambda$, where λ and $\Delta\lambda$ are the central emission wavelength and FWHM, respectively. Under optical pumping of 17.5 kW/cm^2, the Q factor is 77, which is fairly high considering the length of our nanocavity. From the "s" shaped L-L curve, the β factor, defined as the fraction of spontaneous emission coupled into the lasing mode, can be determined. Based on the evaluation of the ratio of output intensity below and above the threshold[23], the β factor of 0.76 has been obtained for our sample.

For comparison and also as a reference, another separate InGaN/GaN nanorod fabricated in the same batch and deposited on the SiO$_2$ surface but without silver underneath does not exhibit any lasing behaviour even under an optical pumping of up to 17.5 kW/cm^2 as shown Fig. 3a and 3b. In these figures the emission spectrum and the FWHM of the emission peak as a function of excitation power density are given, respectively. Fig. 3a and 3b only show broad spontaneous emission peaks with slightly increased FWHM of the emission peak with increasing the optical pumping power density. The lasing of our plasmonic laser at 431 nm (Fig. 2a) exhibits a 5 nm blue-shift compared to the bare nanorod sample (Fig. 3a), showing a frequency pulling effect[24]. From gain = loss = 2nπ/c × ($\Delta\nu$) under steady state conditions, where n and $\Delta\nu$ are refractive index and FWHM, respectively[25], the gain and loss can be estimated to 4.3×10^3 cm^{-1}, which is close to the gain stated above.
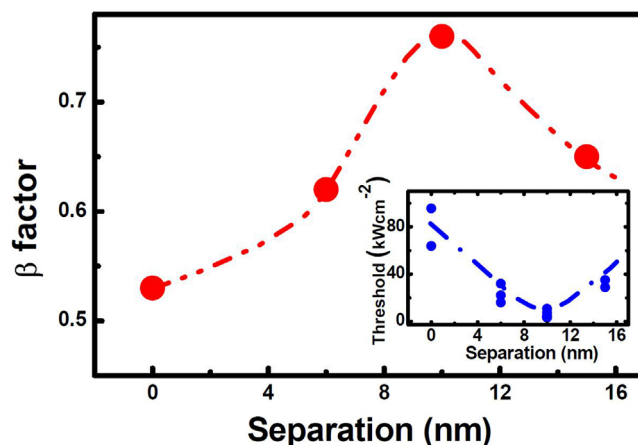
It is worth highlighting that the integrated intensity of our nano-SPASER as shown in Fig. 2a is more than 9 times higher than that of spontaneous emission both under an excitation power density of 10.5 kW/cm^2. The great enhancement is ascribed to strong SP coupling.
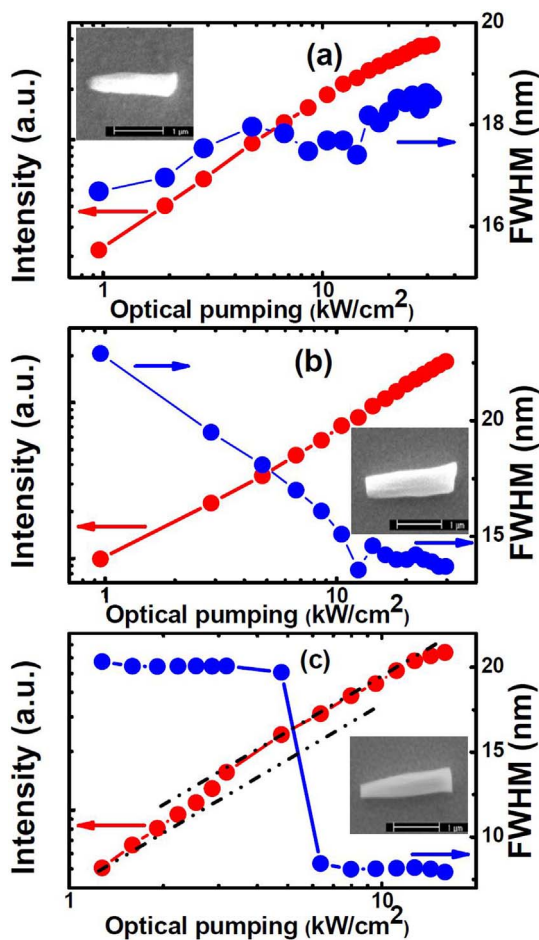
Figure 4 | **SEM images of different kinds of nanorods and their optical characteristics (L-L plot and linewidth as a function of optical pumping) for (a) Nanorod without either parallel facets or straight side-walls; (b) Nanorod with non-parallel facets; and (c) Nanorod with parallel facets and fairly straight side-walls. The dash-lines are guides to eyes.**

Figure 5 | **β factor of our nano-SPASERs as a function of the thickness of SiO$_2$ spacer between the InGaN/GaN MQWs and the silver film.** The inset figure shows the thresholds as a function of the SiO2 thickness. The dash-lines are guides to eyes.

In fact, we have observed two lasing peaks at different modes, one at 431 nm described above, and another at 449 nm, as shown in Fig. 2a. The latter shows identical behaviour to the one at 431 nm. Based on the GaN refractive index of 2.55 and the nanorod length (i.e., the F-P cavity length), the mode spacing is approximately 18 nm. By carefully examining Fig. 2a, there is an extra peak with a weak emission at 468 nm, which is 19 nm longer than the second lasing peak at 449 and 37 nm longer than the 1st lasing peak at 431 nm. Apparently, the optical modes at 431 and 449 nm are within the gain spectral region and thus obtain sufficient gain to generate lasing, while the mode at 468 nm cannot obtain enough gain as it is out of the gain spectral region.

We have also found that the nanorod morphology and the quality of the facets play an important role in achieving lasing with a low threshold in cw mode at room temperature, as shown in Fig. 4. For example, the nanorod shown in the inset of Fig. 4a does not produce a good F-P cavity, as it does not exhibit good uniformity in diameter across the length of the nanorod and the facets at each end are not so parallel and smooth. Consequently, both the L-L plot and the FWHM of the emission peaks as a function of optical pumping power density (Fig. 4a) confirm that no lasing behaviour is observed. The inset of Fig. 4b shows a different nanorod with a good facet at one end only. Compared with the nanorod as shown in Fig. 4a, the uniformity in diameter has been improved. Fig. 4b indicates that the sample exhibits a clear narrowing in FWHM of the emission

peak, but the L-L plot shows weak superlinear behaviour. This demonstrates a weak feature of amplified spontaneous emission (ASE)[26], but not clear lasing. The inset of Fig. 4c exhibits another nanorod with a pair of parallel and smooth facets and further improved uniformity in diameter, showing a clear "s" shaped L-L plot and a dramatic reduction in FWHM of the emission peak, the fingerprints for lasing behaviour. The threshold for the sample is only slightly higher than 3.5 kW/cm² for the nanorod discussed above, demonstrating an excellent reproducibility of our fabrication of nano-SPASER.

In order to further support the above conclusion, we fabricated a separate nano-SPASER structure as a reference, where the thick SiO$_2$ layer (~300 nm) on the top of the nanorod has not been removed during the fabrication process. (See supplementary information for the details of the fabrication, where the thick SiO$_2$ is initially deposited on the as-grown epi-wafer as a mask for the subsequent fabrication of nanorod arrays). Under identical measurement conditions to those used above, the L-L curve and the FWHM as a function of optical pumping power density have been obtained (not shown). This allows the determination of a threshold of 11.5 kW/cm² for lasing, which is 3 times higher that that of the above nano-SPASER without the SiO$_2$ on its top as shown in Fig. 2a. Furthermore, the Q-factor of the sample with the SiO$_2$ also drops down to 63. The increased threshold is attributed to the reduced reflectance at the facets as a result of the SiO$_2$ on the top. (See supplementary information).

Taking advantage of the accurate control over the separation between the InGaN quantum wells and the silver in our nano-SPASER geometry, we have fabricated a set of samples with different thickness of SiO$_2$ spacer layer (0, 6, 10 and 15 nm) in order to study the impact of the separation on the β factor and threshold. Fig. 5 shows the β factor as a function of the separation between the InGaN MQWs and the silver film, which is actually the thickness of the SiO$_2$ spacer. Fig. 5 indicates that a 10 nm SiO$_2$ spacer would be the best to achieve the highest β factor. For large separations, the β factor is reduced as the local field enhancement due to the SP coupling is weak due to the evanescent nature. On the opposite side, which is the case of very small separation, the efficiency of non-radiative energy transfer loss is enhanced, and thus non-radiative quenching is increased. As a result, the β factor decreases with separation[27–29]. Therefore, the sample with a 10 nm spacer exhibits the highest β factor, corresponding to the lowest threshold as shown in the inset of Figure 5.

In summary, we demonstrated a plasmonic nanolaser fabricated using an InGaN/GaN MQW based LED structure by means of a post-growth approach. It is the first semiconductor based plasmonic nanolaser which works at room temperature in cw mode so far. The laser operates at an ultralow threshold with a high β value and strong mode confinement in subwavelength scales. As the nanorods were fabricated by a simple top-down method on a standard LED epitaxial wafer which contains both n- and p-type doping layers, it therefore offers the potential for the fabrication of an electrically pumped SPASER in future. We believe that this work paves the way for the fabrication of ultra-small lasers which will be applied to future advanced on-chip integrated optical circuits.

Methods

Nanorods fabrication. The nanorods were fabricated from a standard LED epi-wafer, which was grown by MOCVD on a c-plane sapphire substrate. The epi-wafer consists of 1 μm undoped GaN followed by a 25 nm low-temperature nucleation layer, a 2.8 μm thick n-GaN layer, then 10 pairs of GaN/In$_x$Ga$_{1-x}$N MQWs with barrier and well thickness of 2.9 and 13.4 nm respectively, a 30 nm thin Al$_x$Ga$_{1-x}$N electron blocking layer, and finally a 200 nm p-GaN layer. The epi-wafer was then fabricated into nanorod array structure by a top-down dry etching method using our self-organised nickel as nanomasks. Compared with the direct growth approaches on silicon, the post-growth fabrication approach exhibits major advantages in terms of reproducibility, enhanced performance and great potential for scale-up[30,31]. The detailed process for the fabrication of our InGaN/GaN nanorods is schematically shown in Supplementary Fig. S1.

Fabrication of a plasmonic waveguide. Metal/dielectric layer was fabricated on a Si substrate. A 500 nm thick SiO$_2$ layer was firstly grown on a pre-cleaned Si substrate by plasma enhanced chemical vapour deposition (PECVD). Subsequently, a silver film with a thickness of 85 nm was deposited on the SiO$_2$ with a deposition rate of 0.1 nm/s by thermal evaporator under a background pressure of less than 2×10^{-6} mbar. Afterwards, a SiO$_2$ spacer was deposited by using an electron-beam evaporator under a vacuum of less than 5×10^{-6} mbar. The surface roughness was measured by AFM (see Supplementary Fig. S3).

Nano-SPASER fabrication. The nanorods were cleaved from the substrate with a diamond cutter into an IPA solution. The nanorods/IPA suspension was then obtained using a centrifuge, and subsequently the nanorods were transferred onto the prepared SiO$_2$ dielectric on the silver film as stated above using a drop casting method. The distribution of nanorods was examined by SEM, showing a number of coffee rings consisting of a large number of nanorods (see Supplementary Fig. S4), frequently observed using the drop casting method[32]. Individual nanorods can be easily found in the region between the coffee rings. Before transferring onto the substrates, the nanorods undergo a surface treatment involving the utilisation of hot nitric acid in order to remove the residual etchants and the damage generated during the dry etching process.

Measurements. Standard photoluminescence (PL) measurements were carried out with a 375 nm diode laser as excitation source and a monochromator (Horiba SPEX 500 M) equipped with an air-cooled charge coupled device (CCD). For the lasing spectrum measurement, a micro-PL system was used, with a 405 nm cw diode laser as an excitation source. An objective lens (50×, NA = 0.43) was used to focus the laser beam down to a spot with a diameter < 2 μm. The emission spectra were recorded by a monochromator (Horiba iHR550) with a resolution of 0.1 nm together with an air-cooled CCD. All the measurements were performed at room temperature.

1. Rong, H. *et al.* A continuous-wave Raman silicon laser. *Nature* **433**, 725–728 (2005).
2. Hirschman, K. D., Tsybeskov, L., Duttagupta, S. P. & Fauchet, P. M. Silicon-based visible light-emitting devices integrated into microelectronic circuits. *Nature* **384**, 338–341 (1996).
3. Oulton, R. F., Sorger, V. J., Genov, D. A., Pile, D. F. P. & Zhang, X. A hybrid plasmonic waveguide for sub-wavelength confinement and long-range propagation. *Nat. Photonics* **2**, 496–500 (2008).
4. Bergman, D. J. & Stockman, M. I. Surface plasmon amplification by stimulated emission of radiation: quantum generation of coherent surface plasmons in nanosystems. *Phys. Rev. Lett.* **90**, 027402 (2003).
5. Noginov, M. A. *et al.* Demonstration of a spaser-based nanolaser. *Nature* **460**, 1110–1112 (2009).
6. Oulton, R. F. *et al.* Plasmon lasers at deep subwavelength scale. *Nature* **461**, 629–632 (2009).
7. Ma, R. M., Oulton, R. F., Sorger, V. J., Bartal, G. & Zhang, X. Room-temperature sub-diffraction-limited plasmon laser by total internal reflection. *Nat. Mater.* **10**, 110–113 (2011).
8. Wu, C. Y. *et al.* Plasmonic green nanolaser based on a metal–oxide–semiconductor structure. *Nano Lett.* **11**, 4256–4260 (2011).
9. Lu, Y. J. *et al.* Plasmonic nanolaser using epitaxially grown silver film. *Science* **337**, 450–453 (2012).
10. Sobanska, M. *et al.* Plasma-assisted MBE growth of GaN on Si(111) substrates. *Cryst. Res. Technol* **47**, 307–312 (2012).
11. Okamoto, K., Niki, I., Shvartser, A., Narukawa, Y., Mukai, T. & Scherer, A. Surface-plasmon-enhanced light emitters based on InGaN quantum wells. *Nat. Mater.* **3**, 601–605 (2004).
12. Kwon, M. K. *et al.* Surface-plasmon-enhanced light-emitting diodes. *Adv. Mater.* **20**, 1253–1257 (2008).
13. Nezhad, M. P. *et al.* Room-temperature subwavelength metallo-dielectric lasers. *Nat. Photonics* **4**, 395–399 (2010).
14. Khajavikhan, M. *et al.* Thresholdless nanoscale coaxial lasers. *Nature* **482**, 204–207 (2012).
15. Bai, J., Wang, Q. & Wang, T. Characterization of InGaN-based nanorod light emitting diodes with different indium compositions. *J. Appl. Phys.* **111**, 113103 (2012).
16. Dawson, P., Puygranier, B. A. F. & Goudonnet, J. P. Surface plasmon polariton propagation length: A direct comparison using photon scanning tunneling microscopy and attenuated total reflection. *Phys. Rev. B* **63**, 205410 (2001).
17. Zhao, H. & Tansu, N. Optical gain characteristics of staggered InGaN quantum wells lasers. *J. Appl. Phys.* **107**, 113110 (2010).
18. Dworzak, M. *et al.* Gain mechanisms in field-free InGaN layers grown on sapphire and bulk GaN substrate. *phys. stat. sol. (RRL)* **1**, 141–143 (2007).
19. Wang, Q., Bai, J., Gong, Y. P. & Wang, T. Influence of strain relaxation on the optical properties of InGaN/GaN multiple quantum well nanorods. *J. Phys. D: Appl. Phys.* **44**, 395102 (2011).
20. Ramesh, V., Kikuchi, A., Kishino, K., Funato, M. & Kawakami, Y. Strain relaxation effect by nanotexturing InGaN/GaN multiple quantum well. *J. Appl. Phys.* **107**, 114303 (2010).
21. Liu, B., Smith, R., Bai, J., Gong, Y. & Wang, T. Great emission enhancement and excitaonic recombination dynamic of InGaN/GaN nanorod structures. *Appl. Phys. Lett.* **103**, 101108 (2013).
22. Zhao, H., Arif, R. A., Ee, Y. K. & Tansu, N. Optical gain and spontaneous emission of strain-compensated InGaN-AlGaN quantum wells including carrier screening effect. *Proc. of SPIE* **6889**, 688903 (2008).
23. Li, K. H., Ma, Z. & Choi, H. W. High-Q whispering-gallery mode lasing from nanosphere-patterned GaN nanoring arrays. *Appl. Phys. Lett.* **98**, 071106 (2011).
24. Allaria, E., De Ninno, G. & Spezzani, C. Experimental demonstration of frequency pulling in single-pass free-electron lasers. *Opt. Express* **19**, 10619–10624 (2011).
25. Saleh, B. E. A. & Teich, M. C. Fundamental of photonics (1st edition, John Wiley & Sons, Inc.). 502–503 (1990).
26. Zimmler, M. A., Bao, J., Capasso, F., Müller, S. & Ronning, C. Laser action in nanowires: Observation of the transition from amplified spontaneous emission to laser oscillation. *Appl. Phys. Lett.* **93**, 051101 (2008).
27. Linic, S., Christopher, P. & Ingram, D. B. Plasmonic-metal nanostructures for efficient conversion of solar to chemical energy. *Nat. Mater.* **10**, 911–921 (2011).
28. Sorger, V. J. *et al.* Strongly enhanced molecular fluorescence inside a nanoscale waveguide gap. *Nano Lett.* **11**, 4907–4911 (2011).
29. Anger, P., Bharadwaj, P. & Novotny, L. Enhancement and quenching of single-molecule fluorescence. *Phys. Rev. Lett.* **96**, 113002 (2006).
30. Bae, S. Y., Dong, D. J., Lee, J. Y., Seo, D. J. & Lee, D. S. Size-controlled InGaN/GaN nanorod array fabrication and optical characterization. *Opt. Express* **21**, 16854–16862 (2013).
31. Li, S. & Waag, A. GaN based nanorods for solid state lighting. *J. Appl. Phys.* **111**, 071101 (2012).
32. Sun, P. *et al.* Suppression of the coffee-ring effect by self-assembling graphene oxide and monolayer titania. *Nanotechnology* **24**, 075601 (2013).

Acknowledgments

Author contributions

T.W. proposed and designed the whole experiments, carried out the analysis, wrote the manuscript, and organised this research project; Y.H. and P.R. fabricated the samples, performed optical measurements, prepared part of the figures, and were involved in data analysis and preparing the manuscript; B.L. helped Y.H. perform optical measurements and was involved in data analysis; J.B. was involved in helping Y.H. fabricate the samples.

Additional information